Generating Optical Orbital Angular Momentum in a High-Gain Free-Electron Laser at the First Harmonic

E. Hemsing, A. Marinelli, and J. B. Rosenzweig

Particle Beam Physics Laboratory, Department of Physics and Astronomy, University of California Los Angeles, Los Angeles, California 90095, USA

(Received 6 December 2010; published 22 April 2011)

A scheme to generate intense coherent light that carries orbital angular momentum (OAM) at the fundamental wavelength of an x-ray free-electron laser (FEL) is described. The OAM light is emitted as the dominant mode of the system until saturation provided that the helical microbunching imposed on the electron beam is larger than the shot-noise bunching that leads to self-amplified emission. Operating at the fundamental, this scheme is more efficient than alternate schemes that rely on harmonic emission, and can be applied to x-ray FELs without using external optical mode conversion elements.

DOI: 10.1103/PhysRevLett.106.164803 PACS numbers: 41.60.Cr, 41.50.+h, 42.50.Tx, 42.65.Ky

It is well known that modes of light can carry effective orbital angular momentum (OAM) due to an azimuthal component of the linear photon momentum that is manifested as a helical phase dependence [1]. OAM light has become both a subject of intense research as well as a useful tool in research [2–5]. In addition to applications in subdiffraction limit microscopy [6], imaging [7] and optical pump schemes [8], OAM light can also be used to probe matter in new ways by imparting a torque from the constituent photons. These critical new aspects of coherent light pulses may be exploited at short wavelength in frontier hard x-ray free-electron lasers (FELs) that have the ability to examine Å length and femtosecond time scales [9]. X rays with OAM have been proposed for research in scattering and spectroscopy [10], chirality in biological materials [11], and quadrupolar transitions in materials due to strong dichroic properties [12].

Traditionally, OAM light has been generated by inserting optical elements into the light path. Some of these techniques have been used to create optical vortices at x-ray wavelengths [13], but at the high peak intensities (10^{18} W/cm^2) associated with modern hard x-ray FELs, such direct optical manipulations may not be practical or available. OAM light generation in an FEL has been explored previously in the context of higher-harmonic emission from a helical undulator [14], and been observed experimentally in nonlinear harmonic generation (NHG) setups where the *e* beam emits frequency harmonics in an undulator due to strong nonlinear microbunching [15]. However, because radiation at the fundamental frequency dominates, such harmonic light emission methods rely either on external spectral filters or on other techniques to suppress the fundamental interaction [16] in order to isolate the OAM light. As an alternative approach, in this Letter we investigate an efficient scheme that generates intense OAM light in an FEL operating at the fundamental frequency. The technique may be designated as high-gain high-mode generation (HGHMG), wherein the source electron beam (*e*-beam) distribution is prearranged so that it radiates transverse higher-order optical modes of the FEL. As a prebunched beam will emit coherent light with a phase structure determined by the microbunching distribution, a helically microbunched beam will emit light with a helical phase and a corresponding value of OAM. Because the light is emitted directly from the *e* beam, this eliminates the need for external mode conversion elements. It also provides a technique by which OAM can be generated with a high degree of spatial coherence, high power and at an extremely wide range of wavelengths, by virtue of the broad flexibility of FEL devices. This may be of general interest for fundamental research on OAM light, higher-order *e*-beam-radiation interactions, or of practical interest for FEL users who require higher-order optical modes.

OAM light generation in an FEL using a helically modulated *e* beam was initially suggested in [17], and the method to produce the highly correlated helical electron beam density distribution was described in [18] for low energies. Here we examine a practical and promising variant scheme optimized for x-ray and VUV wavelengths, which is where the most compelling modern applications of FELs are found. A layout is shown in Fig. 1 and is summarized as follows. An initially unmodulated relativistic *e* beam is helically modulated in energy in a helical undulator (modulator), seeded by a laser (seed laser) tuned to a harmonic *h* of the resonant interaction. The *e* beam is

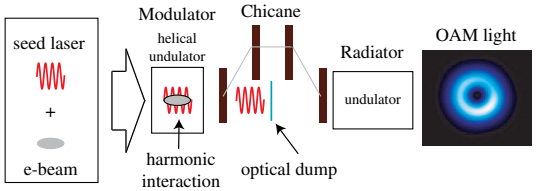

FIG. 1 (color online). Arrangement for generating OAM light in an FEL.

then sent into a longitudinally dispersive section which converts the energy modulation into a helical density modulation, and is finally sent into an undulator (radiator) where the helically microbunched e beam radiates coherent OAM light. With a transversely Gaussian input seed laser profile, the index of the radiated OAM mode is $l = \mp n(h-1)$ where n is the frequency harmonic of the emission. At $n = 1$, the radiator output has the same frequency as the modulating Gaussian seed laser, but acquires an OAM value of $l = \mp(h-1)$. Further, for $n \geq 2$, NHG schemes used in tandem with the HGHMG scheme can produce frequency harmonic emission in the radiator with correspondingly larger values of OAM.

Consider the transverse electric field of the modulator's seed laser (Fig. 1) which is assumed to have a pulse length long compared to the e-beam bunch length. It has the form $\mathbf{E}(\mathbf{x}, t) = \mathrm{Re}[\tilde{E}(\mathbf{x})\hat{\mathbf{e}}_\perp e^{ik(z-ct)}]$, where $\hat{\mathbf{e}}_\perp$ is a unit vector specifying the direction of polarization, $k = 2\pi/\lambda$ is the radiation wave number and $\tilde{E}(\mathbf{x})$ is the slowly growing complex field amplitude which here is taken to be a single free-space mode. The time-averaged electromagnetic power is $P = (2\mu_0 c)^{-1}\int|\tilde{E}(\mathbf{x})|^2 d^2\mathbf{x}$. Harmonic motion is generated when the electron interacts with the gradients in the field. The portion of the field contributing to the harmonic interaction in the modulator is found by Taylor expansion of the field experienced by an electron about its centroid position. In a helical modulator with field polarization $\hat{\mathbf{e}}_w = (\hat{\mathbf{e}}_x \pm i\hat{\mathbf{e}}_y)/\sqrt{2}$, corresponding to right (+) or left (−) circular polarization along z, the lowest-order harmonic field terms experienced at the electron position are given by [18],

$$\tilde{E}^{(h)}(\mathbf{x}) = \frac{1}{(h-1)!}\left[\frac{\pm i\bar{K}}{2k_w\gamma}e^{\mp i\phi}(\partial_r \mp \frac{i}{r}\partial_\phi)\right]^{h-1}\tilde{E}(\mathbf{x}), \tag{1}$$

where h is the harmonic number. The wiggling amplitude is assumed small compared to the transverse e-beam size. The change in energy of an electron in the beam as it interacts with the fields of the modulator and laser near the harmonic resonance is given by

$$\frac{d\eta}{dz} = \frac{e\bar{K}}{\sqrt{2}\gamma^2 mc^2}\mathrm{Re}[ig_\perp\tilde{E}^{(h)}(\mathbf{x})e^{i\psi_0^{(h)}}] \tag{2}$$

where $\eta = (\gamma - \gamma_0)/\gamma_0 \ll 1$ is the relative energy deviation of the electron from the resonant energy $\gamma_0 = \sqrt{(1+\bar{K}^2)k/2hk_w}$, $\gamma_z^2 = \gamma^2/(1+\bar{K}^2) = (1-\beta_z^2)^{-1}$ is the longitudinal relativistic factor, $\bar{K} = eB/mck_w$ is the rms undulator parameter and $k_w = 2\pi/\lambda_w \ll k$ is the wave number of the modulator magnetic field. Polarization alignment between the light and the direction of e-beam motion through the modulator is given by $g_\perp = 1$ if the input field is properly circularly polarized, or $g_\perp = 1/\sqrt{2}$ if it is linearly polarized. The harmonic ponderomotive phase is $\psi_0^{(h)} = kz + hk_w z - ckt$ which, in combination with the phase terms in (1) shows that the resonant (ponderomotive) field component in the modulator section has an azimuthal dependence of the form $\exp[\mp i(h-1)\phi]$. Thus, the electrons in the resonant bucket experience an energy modulation that depends on their azimuthal position at harmonics $h > 1$.

In general, $\tilde{E}(\mathbf{x})$ is a free-space laser field with a spot size and phase that can vary along the modulator. The Rayleigh lengths associated with the short wavelengths of interest, however, may be considered to be much longer than the modulator length L_m, so for simplicity the field is approximated as a simple Gaussian $\tilde{E}(\mathbf{x}) = 2\sqrt{\mu_0 cP/\pi w_0^2}\exp(-r^2/w_0^2)$. We concentrate on the second harmonic of the modulator ($h = 2$), where the ponderomotive field amplitude in Eq. (1) is,

$$\tilde{E}^{(2)}(r,\phi) = \frac{\mp 2i\bar{K}r}{\gamma k_w w_0^3}\sqrt{\frac{P\mu_0 c}{\pi}}e^{\mp i\phi - r^2/w_0^2}, \tag{3}$$

and has an azimuthal phase dependence $\mp(h-1)\phi = \mp\phi$. Linearizing Eq. (2) to first order for small modulations, the relative electron energy at the modulator exit is

$$\eta = \eta_0 \pm a(r)\cos(k_b s_0 \mp \phi), \tag{4}$$

where η_0 is the initial relative energy, $s_0 = z - \beta_z ct$ is the initial co-moving beam coordinate, $k_b = k/\beta_z$ is the microbunching wave number, and

$$a(r) = \frac{g_\perp e\bar{K}^2 L_m r}{\gamma^3 mc^2 k_w w_0^3}\sqrt{\frac{2P\mu_0 c}{\pi}}e^{-r^2/w_0^2}. \tag{5}$$

The energy modulation in the beam has the shape of a single twist "spiral-staircase" via the phase dependence on ϕ, with the electrons near the axis unmodulated (Fig. 2).

Unlike the single-stage scheme in [18], the high e-beam energies associated with x-ray FELs require use of a longitudinally dispersive section (e.g. a chicane) to convert the helical energy modulation into a helical density modulation for OAM emission in the radiator. The simple dispersive section is characterized by the transport matrix

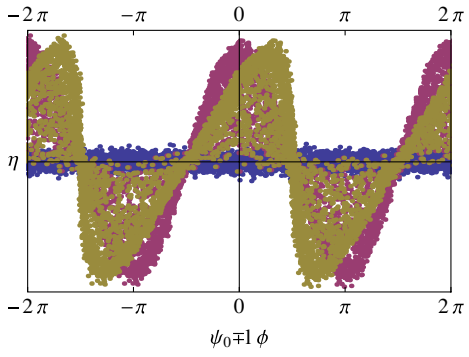

FIG. 2 (color online). Initially unmodulated e beam (blue) becomes helically modulated in energy during the harmonic interaction (red), and is helically density bunched (tan) after transit through the dispersive section.

element $R_{56} = \partial s_0/\partial\eta$ which maps the longitudinal beam coordinate s_0 at the entrance into s, the beam coordinate at the exit, via $s = s_0 + R_{56}\eta$. The helical microbunching factor of the distribution f after the dispersive section is

$$b_l(k') = \left\langle \int f(r, \eta, \phi, s) e^{-ik's - il\phi} r dr d\eta d\phi \right\rangle, \quad (6)$$

which quantifies the density modulation into the discrete helical mode l at the wave number k'. The brackets represent averaging over s, defined as $\langle \ldots \rangle = \lim_{2L\to\infty} \frac{1}{2L} \times \int_{-L}^{L} (\ldots) ds$. The final variables transform into the initial variables via $f ds d\eta = f_0 ds_0 d\eta_0$, where $f_0(r, \eta_0)$ is an unmodulated axisymmetric initial distribution function that satisfies $\int f_0 r dr d\eta_0 d\phi = 1$. For a beam much longer than the microbunching wavelength the bunching factor at the exit of the chicane is peaked about $k' = nk_b$ where $n \geq 1$ is the harmonic number associated with the microbunching structure. In terms of initial variables (6) is,

$$|b_l(k_b)| = \left| 2\pi\delta_{n,\mp l} \int f_0 e^{-ink_b R_{56}\eta_0} J_n[nk_b R_{56} a] r dr d\eta_0 \right|. \quad (7)$$

The Kronecker delta factor $\delta_{n,\mp l}$ shows how the excited helical mode index, l, relates to the harmonic number, n for the present case of $h = 2$. At the fundamental microbunching frequency, $k' = k_b$, the only azimuthal mode that is nonzero is $l = -1(1)$ for the right- (left-) circularly polarized modulator.

Consider an initially uncorrelated Gaussian beam distribution $f_0 = (2\pi\sigma_x^2\sqrt{2\pi\sigma_\eta^2})^{-1} \exp(-r^2/2\sigma_x^2 - \eta_0^2/2\sigma_\eta^2)$ where σ_η is the relative rms energy spread and σ_x is the transverse rms beam size. The bunching amplitude, which carries a Gaussian suppression factor due to the energy spread, is then

$$|b_l| = \delta_{n,\mp l} e^{-(nk_b R_{56}\sigma_\eta)^2/2} |\Gamma_n|, \quad (8)$$

where $\Gamma_n = \sigma_x^{-2} \int \exp(-r^2/2\sigma_x^2) J_n(2nA\frac{r}{\sigma_x} e^{-r^2/w_0^2}) r dr$ and

$$A = \frac{2g_\perp e\bar{K}^2 R_{56} L_m \sigma_x}{\gamma_0 mc^2(1+\bar{K}^2) w_0^3} \sqrt{\frac{2P\mu_0 c}{\pi}}. \quad (9)$$

Two limits yield useful simplifications for the contribution of transverse parameters in Γ_n; with $A \ll 1$ the radial integral gives $\Gamma_n = \frac{(\sqrt{2}nA)^n (n/2)!}{n!} (1 + 2n\sigma_x^2/w_0^2)^{-(n+2)/2}$, and maximal density bunching is obtained with $R_{56} = (\sqrt{n} k_b \sigma_\gamma)^{-1}$. Alternatively, in the large laser spot limit of $w_0 \gg 2\sigma_x$, the radial integral gives $\Gamma_n = \frac{(\sqrt{2}nA)^n (n/2)!}{n!} {}_1F_1(\frac{n}{2} + 1, n + 1, -2n^2A^2)$ where ${}_1F_1$ is the confluent hypergeometric function. Figure 3 shows how Γ_1 varies with the parameter A in general.

Imprinted with the helical density distribution at the chicane exit, the e beam then enters the radiating undulator (with any polarization) with period $\lambda_{w,r}$ tuned to emit light at the fundamental wavelength of the microbunching

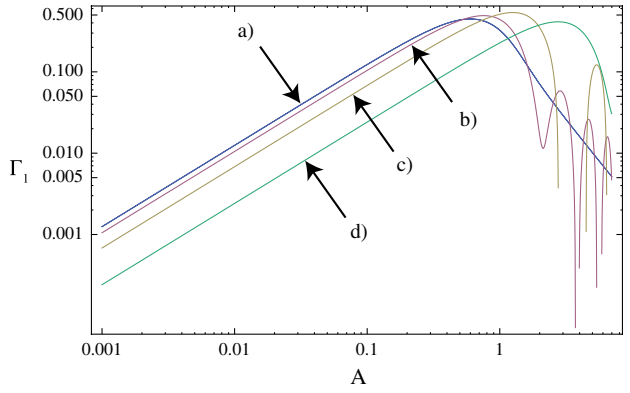

FIG. 3 (color online). Contribution of transverse beam sizes to the $|l| = 1$ helical bunching factor. The ratio of the e-beam size to the rms laser spot size is (a) $2\sigma_x/w_0 \ll 1$, (b) 0.5, (c) 1, and (d) 2.

period: $\lambda_b = 2\pi/k_b = \frac{\lambda_{w,r}}{2\gamma_0^2}(1 + \bar{K}_r^2)$, where $\bar{K}_r$ is the rms undulator parameter of the radiator. For $n = 1$, the OAM emission is at the same wavelength as that of the seed laser in the modulator section, so the entire setup in Fig. 1 acts as a "mode converter" which transforms the initially transversely Gaussian laser pulse into an OAM mode by virtue of the natural manipulation of the e-beam microbunching distribution. Since other modes can by amplified spontaneously due to shot noise in the beam, and because mode competition usually favors the fundamental, the helical bunching factor must be greater than the effective shot-noise bunching factor in the radiator, $b_{SN} \simeq \sqrt{\sqrt{2\pi} ec\rho/9I_0\lambda_b}$ where ρ is the FEL parameter and I_0 is the beam current, to allow for the OAM mode to dominate from the outset. It is also important that the betatron phase advance is minimized through transport in order to preserve the correlated helical structure in the e beam.

Figure 4 shows the power as a function of the azimuthal mode number in the radiation field calculated with time-independent numerical simulations from GENESIS [19] for a Linac Coherent Light Source (LCLS)-type e beam [9] at $\lambda_b = 1.5$ Å. In this $n = 1$, $h = 2$ scenario, virtually all of the power is emitted into the dominant $l = 1$ mode, with less than 1% in the $l = 0$, -1 modes at any

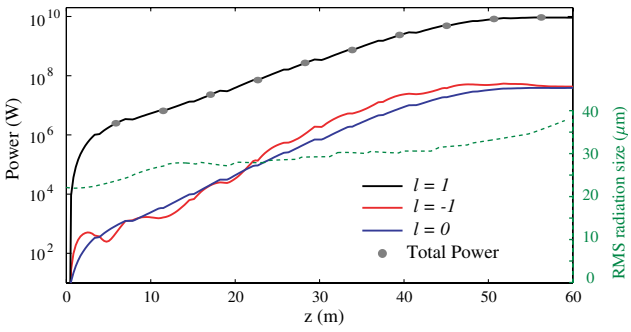

FIG. 4 (color online). Optical power in l modes for beam lasing at 1.5 Å.

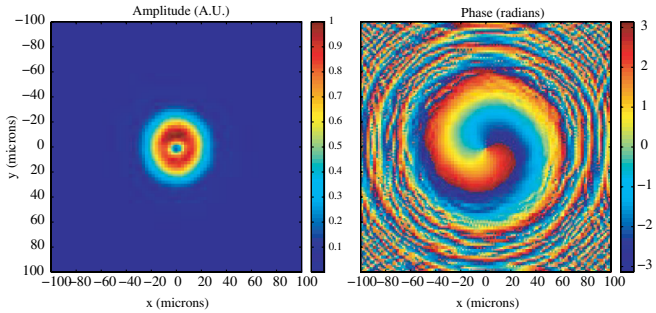

FIG. 5 (color online). Transverse profile of the light reveals a dominant $l = 1$ OAM mode at saturation.

given z position. The characteristic hollow profile and helical phase of the $l = 1$ mode are shown in Fig. 5. The dominance of the $l = 1$ mode over the fundamental is also indicated in the bunching factor of the $l = 0$ beam mode, which stays below 2% throughout. Relevant parameters used are $\gamma_0 = 26\,700$, $\sigma_x = 23$ μm, $\sigma_\eta = 0.01\%$, giving a $b_1 = 1.47\%$ initial bunching factor using a $P = 1$ GW, $w_0 = 31$ μm Gaussian input seed (supplied by the upstream FEL) in a $\bar{K} = 3$, $L_w = 7$ m modulator followed by a small $R_{56} = 0.24$ μm chicane. At this level the bunching factor is much larger than the effective shot-noise bunching $b_{\mathrm{SN}} \simeq 1.2 \times 10^{-4}$, but is small enough that the coherent OAM emission develops into high-gain amplification with an average gain length of 4.5 m before saturating after 50 m. The e beam emits $P_{\mathrm{out}} = 10$ GW of OAM light through a linearly polarized LCLS-type undulator with $\bar{K}_r = 2.47$, $\lambda_{w,r} = 3$ cm at a beam current of $I_0 = 3$ kA and normalized emittance $\epsilon_{\mathrm{nx}} = 0.5$ μm. Note that with $P_{\mathrm{out}}/P = 10$, the HGHMG scheme acts as a combination mode-converter and amplifier of the Gaussian FEL seed laser, delivering an OAM mode describable in mechanical terms as having an available integrated torque about the propagation axis of $\tau = lP_{\mathrm{out}}/kc = 0.8 \times 10^{-9}$ N m.

The HGHMG scheme in this example is seeded by an attenuated x-ray laser pulse similar in character to the output of the LCLS [9] itself. The timing between the Gaussian x-ray FEL laser seed pulse and the e beam in the helical modulator section suggest a self-seeded running scenario to modulate the e-beam; using either a single e beam [20], or better a two-beam self-seeded scheme [21] in which two e beams are separated with a precise delay by correct excitation of the photocathode electron source. The two-beam approach has the advantage of drastically reducing the footprint of the chicane required to sync the seed pulse (emitted by the first beam in the upstream FEL) with the second e beam in the modulator. It can also be employed in tandem with a kicker to impart a large betatron amplitude to the second e beam so that it does not lase in the upstream seed FEL undulator. In this way, the energy spread and microstructure of the e beam is preserved for the downstream helical modulator and OAM radiator stations. In self-seeding, the seed laser passes through an optical delay line that can also be equipped with either a reflective or transmissive monochromator [22] to lengthen the seed pulse and increase the temporal overlap with the e beam in the modulator. When the length of the coherent seed is greater than that of the e-beam bunch, the helical modulation is in phase across the entire bunch and full longitudinal coherence in the emitted OAM mode is obtained. Monochromatization comes at the expense of the seed power, so optimization of this type of setup depends on the available FEL seed power and bandwidth; this is a topic left for future studies. We note also that for pump-probe-type experiments that rely on different optical modes, the optical dump that blocks the seed light can be removed such that the initial Gaussian laser also exits through the second radiator. Since it exits prior to the OAM light pulse at a fixed delay, the setup is that of a two-pulse, two-mode system of a Gaussian beam followed by an OAM beam.

The author E. H. gratefully thanks Z. Huang for helpful discussions. This research is supported by grants from Department of Energy Contract Nos. DOE DE-FG02-07ER46272 and DE-FG03-92ER40693 and Office of Naval Research Contract No. ONR N00014-06-1-0925.

[1] L. Allen *et al.*, Phys. Rev. A **45**, 8185 (1992).
[2] G. Gibson *et al.*, Opt. Express **12**, 5448 (2004).
[3] E. Yao *et al.*, Opt. Express **14**, 13089 (2006).
[4] M. F. Andersen *et al.*, Phys. Rev. Lett. **97**, 170406 (2006).
[5] A. Alexandrescu, D. Cojoc, and E. DiFabrizio, Phys. Rev. Lett. **96**, 243001 (2006).
[6] P. Török and P. Munro, Opt. Express **12**, 3605 (2004).
[7] B. Jack *et al.*, Phys. Rev. Lett. **103**, 083602 (2009).
[8] J. W. R. Tabosa and D. V. Petrov, Phys. Rev. Lett. **83**, 4967 (1999).
[9] P. Emma *et al.*, Nat. Photon. **4**, 641 (2010).
[10] C. Stamm *et al.*, Phys. Rev. B **81**, 104425 (2010).
[11] R. Raval, Nature (London) **425**, 463 (2003).
[12] M. van Veenendaal and I. McNulty, Phys. Rev. Lett. **98**, 157401 (2007).
[13] Y. Kohmura *et al.*, Appl. Phys. Lett. **94**, 101112 (2009).
[14] S. Sasaki and I. McNulty, Phys. Rev. Lett. **100**, 124801 (2008).
[15] E. Allaria *et al.*, Phys. Rev. Lett. **100**, 174801 (2008).
[16] B. W. J. McNeil *et al.*, Phys. Rev. Lett. **96**, 084801 (2006).
[17] E. Hemsing, A. Gover, and J. Rosenzweig, Phys. Rev. A **77**, 063831 (2008).
[18] E. Hemsing *et al.*, Phys. Rev. Lett. **102**, 174801 (2009).
[19] S. Reiche, Nucl. Instrum. Methods Phys. Res., Sect. A **429**, 243 (1999).
[20] J. Feldhaus *et al.*, Opt. Commun. **140**, 341 (1997).
[21] Y. Ding, Z. Huang, and R. D. Ruth, Phys. Rev. ST Accel. Beams **13**, 060703 (2010).
[22] G. Geloni, V. Kocharyan, and E. Saldin, arXiv:1004.4067.